

First Measurement of $f_2'(1525)$ Production in Z^0 Hadronic Decays

DELPHI Collaboration

Abstract

Inclusive production of the $f_2'(1525)$ in hadronic Z^0 decays has been studied in data collected by the DELPHI detector at LEP. The Ring Imaging Cherenkov detectors were important tools in the identification of the decay $f_2'(1525) \rightarrow K^+K^-$. The average number of $f_2'(1525)$ produced per hadronic Z decay,

$$\langle N_{f_2'} \rangle = 0.020 \pm 0.005 \text{ (stat)} \pm 0.006 \text{ (syst)},$$

and the momentum distribution of the $f_2'(1525)$ have both been measured.

(To be submitted to Physics Letters B)

P.Abreu²¹, W.Adam⁵⁰, T.Adye³⁷, E.Agasi³¹, I.Ajinenko⁴², R.Aleksan³⁹, G.D.Alekseev¹⁶, R.Aleman⁴⁹, P.P.Allport²², S.Almehed²⁴, U.Amaldi⁹, S.Amato⁴⁷, A.Andreazza²⁸, M.L.Andrieux¹⁴, P.Antilogus⁹, W-D.Apel¹⁷, Y.Arnoud³⁹, B.Åsman⁴⁴, J-E.Augustin²⁵, A.Augustinus⁹, P.Baillon⁹, P.Bambade¹⁹, F.Barao²¹, R.Barate¹⁴, M.Barbi⁴⁷, G.Barbiellini⁴⁶, D.Y.Bardin¹⁶, A.Baroncelli⁴⁰, O.Barring²⁴, J.A.Barrio²⁶, W.Bartl⁵⁰, M.J.Bates³⁷, M.Battaglia¹⁵, M.Baubillier²³, J.Baudot³⁹, K-H.Becks⁵², M.Begalli⁶, P.Beilliere⁸, Yu.Belokopytov^{9,53}, A.C.Benvenuti⁵, M.Berggren⁴⁷, D.Bertrand², F.Bianchi⁴⁵, M.Bigi⁴⁵, M.S.Bilenky¹⁶, P.Billoir²³, D.Bloch¹⁰, M.Blume⁵², S.Blyth³⁵, T.Bolognese³⁹, M.Bonesini²⁸, W.Bonivento²⁸, P.S.L.Booth²², C.Bosio⁴⁰, S.Bosworth³⁵, O.Botner⁴⁸, E.Boudinou³¹, B.Bouquet¹⁹, C.Bourdarios⁹, T.J.V.Bowcock²², M.Bozzo¹³, P.Branchini⁴⁰, K.D.Brand³⁶, T.Brenke⁵², R.A.Brenner¹⁵, C.Bricman², L.Brillault²³, R.C.A.Brown⁹, P.Bruckman¹⁸, J-M.Brunet⁸, L.Bugge³³, T.Buran³³, T.Burgsmueller⁵², P.Buschmann⁵², A.Buys⁹, S.Cabrera⁴⁹, M.Caccia²⁸, M.Calvi²⁸, A.J.Camacho Rozas⁴¹, T.Camporesi⁹, V.Canale³⁸, M.Canepa¹³, K.Cankocak⁴⁴, F.Cao², F.Carena⁹, L.Carroll²², C.Caso¹³, M.V.Castillo Gimenez⁴⁹, A.Cattai⁹, F.R.Cavallo⁵, L.Cerrito³⁸, V.Chabaud⁹, M.Chapkin⁴², Ph.Charpentier⁹, L.Chaussard²⁵, J.Chauveau²³, P.Checchia³⁶, G.A.Chelkov¹⁶, M.Chen², R.Chierici⁴⁵, P.Chochula⁷, V.Chorowicz⁹, J.Chudoba³⁰, V.Cindro⁴³, P.Collins⁹, J.L.Contreras¹⁹, R.Contri¹³, E.Cortina⁴⁹, G.Cosme¹⁹, F.Cossutti⁴⁶, H.B.Crawley¹, D.Crennell³⁷, G.Crosetti¹³, J.Cuevas Maestro³⁴, S.Czellar¹⁵, E.Dahl-Jensen²⁹, J.Dahm⁵², B.Dalmagne¹⁹, M.Dam²⁹, G.Damgaard²⁹, P.D.Dauncey³⁷, M.Davenport⁹, W.Da Silva²³, C.Defoix⁸, A.Deghorain², G.Della Ricca⁴⁶, P.Delpierre²⁷, N.Demaria³⁵, A.De Angelis⁹, W.De Boer¹⁷, S.De Brabandere², C.De Clercq², C.De La Vaissiere²³, B.De Lotto⁴⁶, A.De Min³⁶, L.De Paula⁴⁷, C.De Saint-Jean³⁹, H.Dijkstra⁹, L.Di Ciaccio³⁸, F.Djama¹⁰, J.Dolbeau⁸, M.Donszelmann⁹, K.Doroba⁵¹, M.Dracos¹⁰, J.Drees⁵², K.-A.Drees⁵², M.Dris³², Y.Dufour⁹, D.Edsall¹, R.Ehret¹⁷, G.Eigen⁴, T.Ekelof⁴⁸, G.Ekspong⁴⁴, M.Elsing⁵², J-P.Engel¹⁰, N.Ershaidat²³, B.Erzen⁴³, M.Espirito Santo²¹, E.Falk²⁴, D.Fassouliotis³², M.Feindt⁹, A.Fenyuk⁴², A.Ferrer⁴⁹, T.A.Filippas³², A.Firestone¹, P.-A.Fischer¹⁰, H.Foeth⁹, E.Fokitis³², F.Fontanelli¹³, F.Formenti⁹, B.Franek³⁷, P.Frenkiel⁸, D.C.Fries¹⁷, A.G.Frodesen⁴, R.Fruhwith⁵⁰, F.Fulda-Quenzer¹⁹, J.Fuster⁴⁹, A.Galloni²², D.Gamba⁴⁵, M.Gandelman⁶, C.Garcia⁴⁹, J.Garcia⁴¹, C.Gaspar⁹, U.Gasparini³⁶, Ph.Gavillet⁹, E.N.Gaziz³², D.Gele¹⁰, J-P.Gerber¹⁰, L.Gerdyukov⁴², M.Gibbs²², R.Gokiel⁵¹, B.Golob⁴³, G.Gopal³⁷, L.Gorn¹, M.Gorski⁵¹, Yu.Gouz^{45,53}, V.Gracco¹³, E.Graziani⁴⁰, G.Grosdidier¹⁹, K.Grzelak⁵¹, S.Gumenyuk^{28,53}, P.Gunnarsson⁴⁴, M.Gunther⁴⁸, J.Guy³⁷, F.Hahn⁹, S.Hahn⁵², Z.Hajduk¹⁸, A.Hallgren⁴⁸, K.Hamacher⁵², W.Hao³¹, F.J.Harris³⁵, V.Hedberg²⁴, R.Henriques²¹, J.J.Hernandez⁴⁹, P.Herquet², H.Herr⁹, T.L.Hessing³⁵, E.Higon⁴⁹, H.J.Hilke⁹, T.S.Hill¹, S-O.Holmgren⁴⁴, P.J.Holt³⁵, D.Holthuizen³¹, S.Hoorelbeke², M.Houlden²², J.Hrubeč⁵⁰, K.Huet³⁹, K.Hultqvist⁴⁴, J.N.Jackson²², R.Jacobsson⁴⁴, P.Jalocha¹⁸, R.Janik⁷, Ch.Jarlskog²⁴, G.Jarlskog²⁴, P.Jarry³⁹, B.Jean-Marie¹⁹, E.K.Johansson⁴⁴, L.Jonsson²⁴, P.Jonsson²⁴, C.Joram⁹, P.Juillot¹⁰, M.Kaiser¹⁷, F.Kapusta²³, K.Karafasoulis¹¹, M.Karlsson⁴⁴, E.Karvelas¹¹, S.Katsanevas³, E.C.Katsoufis³², R.Keranen⁴, Yu.Khokhlov⁴², B.A.Khomenko¹⁶, N.N.Khovanski¹⁶, B.King²², N.J.Kjaer²⁹, H.Klein⁹, A.Klovning⁴, P.Kluit³¹, B.Koene³¹, P.Kokkinias¹¹, M.Koratinos⁹, K.Korcyl¹⁸, V.Kostioukhine⁴², C.Kourkoumelis³, O.Kouznetsov^{13,16}, P.-H.Kramer⁵², M.Krammer⁵⁰, C.Kreuter¹⁷, I.Kronkvist²⁴, Z.Krumstein¹⁶, W.Krupinski¹⁸, P.Kubinec⁷, W.Kucewicz¹⁸, K.Kurvinen¹⁵, C.Lacasta⁴⁹, I.Laktineh²⁵, S.Lanblot²³, J.W.Lamsa¹, L.Lanceri⁴⁶, D.W.Lane¹, P.Langefeld⁵², V.Lapin⁴², I.Last²², J-P.Laugier³⁹, R.Lauhakangas¹⁵, G.Leder⁵⁰, F.Ledroit¹⁴, V.Lefebure², C.K.Legan¹, R.Leitner³⁰, Y.Lemoigne³⁹, J.Lemonne², G.Lenzen⁵², V.Lepeltier¹⁹, T.Lesiak³⁶, D.Liko⁵⁰, R.Lindner⁵², A.Lipniacka³⁶, I.Lippi³⁶, B.Loerstad²⁴, J.G.Loken³⁵, J.M.Lopez⁴¹, D.Loukas¹¹, P.Lutz³⁹, L.Lyons³⁵, J.MacNaughton⁵⁰, G.Maehlum¹⁷, A.Maio²¹, V.Malychev¹⁶, F.Mandi⁵⁰, J.Marco⁴¹, R.Marco⁴¹, B.Marechal⁴⁷, M.Margoni³⁶, J-C.Marin⁹, C.Mariotti⁴⁰, A.Markou¹¹, T.Marou⁵², C.Martinez-Rivero⁴¹, F.Martinez-Vidal⁴⁹, S.Marti i Garcia⁴⁹, J.Masik³⁰, F.Matorras⁴¹, C.Matteuzzi⁹, G.Matthiae³⁸, M.Mazzucato³⁶, M.Mc Cubbin⁹, R.Mc Kay¹, R.Mc Nulty²², J.Medbo⁴⁸, M.Merk³¹, C.Meroni²⁸, S.Meyer¹⁷, W.T.Meyer¹, M.Michelotto³⁶, E.Migliore⁴⁵, L.Mirabito²⁵, W.A.Mitaroff⁵⁰, U.Mjoernmark²⁴, T.Moa⁴⁴, R.Moeller²⁹, K.Moenig⁹, M.R.Monge¹³, P.Moretti¹³, H.Mueller¹⁷, L.M.Mundim⁶, W.J.Murray³⁷, B.Muryn¹⁸, G.Myatt³⁵, F.Naraghi¹⁴, F.L.Navarria⁵, S.Navas⁴⁹, K.Nawrocki⁵¹, P.Negri²⁸, S.Nemecek¹², W.Neumann⁵², N.Neumeister⁵⁰, R.Nicolaidou³, B.S.Nielsen²⁹, M.Nieuwenhuizen³¹, V.Nikolaenko¹⁰, P.Niss⁴⁴, A.Nomerotski³⁶, A.Normand³⁵, M.Novak¹², W.Oberschulte-Beckmann¹⁷, V.Obraztsov⁴², A.G.Olshevski¹⁶, R.Orava¹⁵, K.Osterberg¹⁵, A.Ouraou³⁹, P.Paganini¹⁹, M.Paganoni⁹, P.Pages¹⁰, H.Palka¹⁸, Th.D.Papadopoulou³², K.Papageorgiou¹¹, L.Pape⁹, C.Parkes³⁵, F.Parodi¹³, A.Passeri⁴⁰, M.Pegoraro³⁶, L.Peralta²¹, H.Pernegger⁵⁰, M.Pernicka⁵⁰, A.Perrotta⁵, C.Petridou⁴⁶, A.Petrolini¹³, M.Petrovyck^{28,53}, H.T.Phillips³⁷, G.Piana¹³, F.Pierre³⁹, M.Pimenta²¹, M.Pindo²⁸, S.Plaszczynski¹⁹, O.Podobrin¹⁷, M.E.Pol⁶, G.Polok¹⁸, P.Poropat⁴⁶, V.Pozdniakov¹⁶, M.Prest⁴⁶, P.Privitera³⁸, N.Pukhaeva¹⁶, A.Pullia²⁸, D.Radojicic³⁵, S.Ragazzi²⁸, H.Rahmani³², P.N.Ratoff²⁰, A.L.Read³³, M.Reale⁵², P.Rebecchi¹⁹, N.G.Redaeli²⁸, M.Regler⁵⁰, D.Reid⁹, P.B.Renton³⁵, L.K.Resvanis³, F.Richard¹⁹, J.Richardson²², J.Ridky¹², G.Rinaudo⁴⁵, I.Ripp³⁹, A.Romero⁴⁵, I.Roncagliolo¹³, P.Ronchese³⁶, L.Roos¹⁴, E.I.Rosenberg¹, E.Rosso⁹, P.Roudeau¹⁹, T.Rovelli⁵, W.Ruckstuhl³¹, V.Ruhlmann-Kleider³⁹, A.Ruiz⁴¹, K.Rybicki¹⁸, A.Rybin⁴², H.Saarikko¹⁵, Y.Sacquin³⁹, A.Sadovsky¹⁶, G.Sajot¹⁴, J.Salt⁴⁹, J.Sanchez²⁶, M.Sannino¹³, M.Schimmelpfennig¹⁷, H.Schneider¹⁷, U.Schwickerath¹⁷, M.A.E.Schyns⁵², G.Sciolla⁴⁵, F.Scuri⁴⁶, P.Seager²⁰, Y.Sedykh¹⁶, A.M.Segar³⁵, A.Seitz¹⁷, R.Sekulin³⁷, R.C.Shellard⁶, I.Siccama³¹, P.Siegrist³⁹, S.Simonetti³⁹, F.Simonetto³⁶, A.N.Sisakian¹⁶, B.Sitar⁷, T.B.Skaali³³, G.Smadja²⁵, N.Smirnov⁴², O.Smirnova²⁴, G.R.Smith³⁷, R.Sosnowski⁵¹, D.Souza-Santos⁶, T.Spaso²¹, E.Spiriti⁴⁰, P.Sponholz⁵², S.Squarcia¹³, C.Stanescu⁴⁰, S.Stapnes³³, I.Stavitski³⁶, F.Stichelbaut⁹, A.Stocchi¹⁹, R.Strub¹⁰, B.Stugu⁴, M.Szczekowski⁵¹

M.Szeptycka⁵¹, T.Tabarelli²⁸, J.P.Tavernet²³, E.Tcherniaev⁴², O.Tchikilev⁴², A.Tilquin²⁷, J.Timmermans³¹, L.G.Tkatchev¹⁶, T.Todorov¹⁰, D.Z.Toet³¹, A.Tomaradze², B.Tome²¹, A.Tonazzo²⁸, L.Tortora⁴⁰, G.Transtomer²⁴, D.Treille⁹, W.Trischuk⁹, G.Tristram⁸, A.Trombini¹⁹, C.Troncon²⁸, A.Tsirou⁹, M-L.Turluer³⁹, I.A.Tyapkin¹⁶, M.Tyndel³⁷, S.Tzamarias²², B.Ueberschaer⁵², O.Ullaland⁹, G.Valenti⁵, E.Vallazza⁹, C.Vander Velde², G.W.Van Apeldoorn³¹, P.Van Dam³¹, W.K.Van Doninck², J.Van Eldik³¹, N.Vassilopoulos³⁵, G.Vegni²⁸, L.Ventura³⁶, W.Venus³⁷, F.Verbeure², M.Verlato³⁶, L.S.Vertogradov¹⁶, D.Vilanova³⁹, P.Vincent²⁵, L.Vitale⁴⁶, E.Vlasov⁴², A.S.Vodopyanov¹⁶, V.Vrba¹², H.Wahlen⁵², C.Walck⁴⁴, M.Weierstall⁵², P.Weilhammer⁹, C.Weiser¹⁷, A.M.Wetherell⁹, D.Wicke⁵², J.H.Wickens², M.Wielers¹⁷, G.R.Wilkinson³⁵, W.S.C.Williams³⁵, M.Winter¹⁰, M.Witek¹⁸, K.Woschnagg⁴⁸, K.Yip³⁵, O.Yushchenko⁴², F.Zach²⁵, A.Zaitsev⁴², A.Zalewska¹⁸, P.Zalewski⁵¹, D.Zavrtanik⁴³, E.Zevgolatakos¹¹, N.I.Zimin¹⁶, M.Zito³⁹, D.Zontar⁴³, R.Zuberi³⁵, G.C.Zucchelli⁴⁴, G.Zumerle³⁶

¹Ames Laboratory and Department of Physics, Iowa State University, Ames IA 50011, USA

²Physics Department, Univ. Instelling Antwerpen, Universiteitsplein 1, B-2610 Wilrijk, Belgium and IIHE, ULB-VUB, Pleinlaan 2, B-1050 Brussels, Belgium

and Faculté des Sciences, Univ. de l'Etat Mons, Av. Maistriau 19, B-7000 Mons, Belgium

³Physics Laboratory, University of Athens, Solonos Str. 104, GR-10680 Athens, Greece

⁴Department of Physics, University of Bergen, Allégaten 55, N-5007 Bergen, Norway

⁵Dipartimento di Fisica, Università di Bologna and INFN, Via Irnerio 46, I-40126 Bologna, Italy

⁶Centro Brasileiro de Pesquisas Físicas, rua Xavier Sigaud 150, RJ-22290 Rio de Janeiro, Brazil

and Depto. de Física, Pont. Univ. Católica, C.P. 38071 RJ-22453 Rio de Janeiro, Brazil

and Inst. de Física, Univ. Estadual do Rio de Janeiro, rua São Francisco Xavier 524, Rio de Janeiro, Brazil

⁷Comenius University, Faculty of Mathematics and Physics, Mlynska Dolina, SK-84215 Bratislava, Slovakia

⁸Collège de France, Lab. de Physique Corpusculaire, IN2P3-CNRS, F-75231 Paris Cedex 05, France

⁹CERN, CH-1211 Geneva 23, Switzerland

¹⁰Centre de Recherche Nucléaire, IN2P3 - CNRS/ULP - BP20, F-67037 Strasbourg Cedex, France

¹¹Institute of Nuclear Physics, N.C.S.R. Demokritos, P.O. Box 60228, GR-15310 Athens, Greece

¹²FZU, Inst. of Physics of the C.A.S. High Energy Physics Division, Na Slovance 2, 180 40, Praha 8, Czech Republic

¹³Dipartimento di Fisica, Università di Genova and INFN, Via Dodecaneso 33, I-16146 Genova, Italy

¹⁴Institut des Sciences Nucléaires, IN2P3-CNRS, Université de Grenoble 1, F-38026 Grenoble Cedex, France

¹⁵Research Institute for High Energy Physics, SEFT, P.O. Box 9, FIN-00014 Helsinki, Finland

¹⁶Joint Institute for Nuclear Research, Dubna, Head Post Office, P.O. Box 79, 101 000 Moscow, Russian Federation

¹⁷Institut für Experimentelle Kernphysik, Universität Karlsruhe, Postfach 6980, D-76128 Karlsruhe, Germany

¹⁸Institute of Nuclear Physics and University of Mining and Metallurgy, Ul. Kawiory 26a, PL-30055 Krakow, Poland

¹⁹Université de Paris-Sud, Lab. de l'Accélérateur Linéaire, IN2P3-CNRS, Bât. 200, F-91405 Orsay Cedex, France

²⁰School of Physics and Materials, University of Lancaster, Lancaster LA1 4YB, UK

²¹LIP, IST, FCUL - Av. Elias Garcia, 14-1º, P-1000 Lisboa Codex, Portugal

²²Department of Physics, University of Liverpool, P.O. Box 147, Liverpool L69 3BX, UK

²³LPNHE, IN2P3-CNRS, Universités Paris VI et VII, Tour 33 (RdC), 4 place Jussieu, F-75252 Paris Cedex 05, France

²⁴Department of Physics, University of Lund, Sölvegatan 14, S-22363 Lund, Sweden

²⁵Université Claude Bernard de Lyon, IPNL, IN2P3-CNRS, F-69622 Villeurbanne Cedex, France

²⁶Universidad Complutense, Avda. Complutense s/n, E-28040 Madrid, Spain

²⁷Univ. d'Aix - Marseille II - CPP, IN2P3-CNRS, F-13288 Marseille Cedex 09, France

²⁸Dipartimento di Fisica, Università di Milano and INFN, Via Celoria 16, I-20133 Milan, Italy

²⁹Niels Bohr Institute, Blegdamsvej 17, DK-2100 Copenhagen 0, Denmark

³⁰NC, Nuclear Centre of MFF, Charles University, Areal MFF, V Holesovickach 2, 180 00, Praha 8, Czech Republic

³¹NIKHEF-H, Postbus 41882, NL-1009 DB Amsterdam, The Netherlands

³²National Technical University, Physics Department, Zografou Campus, GR-15773 Athens, Greece

³³Physics Department, University of Oslo, Blindern, N-1000 Oslo 3, Norway

³⁴Dpto. Física, Univ. Oviedo, C/P. Pérez Casas, S/N-33006 Oviedo, Spain

³⁵Department of Physics, University of Oxford, Keble Road, Oxford OX1 3RH, UK

³⁶Dipartimento di Fisica, Università di Padova and INFN, Via Marzolo 8, I-35131 Padua, Italy

³⁷Rutherford Appleton Laboratory, Chilton, Didcot OX11 0QX, UK

³⁸Dipartimento di Fisica, Università di Roma II and INFN, Tor Vergata, I-00173 Rome, Italy

³⁹Centre d'Etudes de Saclay, DSM/DAPNIA, F-91191 Gif-sur-Yvette Cedex, France

⁴⁰Istituto Superiore di Sanità, Ist. Naz. di Fisica Nucl. (INFN), Viale Regina Elena 299, I-00161 Rome, Italy

⁴¹Istituto de Física de Cantabria (CSIC-UC), Avda. los Castros, S/N-39006 Santander, Spain, (CICYT-AEN93-0832)

⁴²Inst. for High Energy Physics, Serpukov P.O. Box 35, Protvino, (Moscow Region), Russian Federation

⁴³J. Stefan Institute and Department of Physics, University of Ljubljana, Jamova 39, SI-61000 Ljubljana, Slovenia

⁴⁴Fysikum, Stockholm University, Box 6730, S-113 85 Stockholm, Sweden

⁴⁵Dipartimento di Fisica Sperimentale, Università di Torino and INFN, Via P. Giuria 1, I-10125 Turin, Italy

⁴⁶Dipartimento di Fisica, Università di Trieste and INFN, Via A. Valerio 2, I-34127 Trieste, Italy

and Istituto di Fisica, Università di Udine, I-33100 Udine, Italy

⁴⁷Univ. Federal do Rio de Janeiro, C.P. 68528 Cidade Univ., Ilha do Fundão BR-21945-970 Rio de Janeiro, Brazil

⁴⁸Department of Radiation Sciences, University of Uppsala, P.O. Box 535, S-751 21 Uppsala, Sweden

⁴⁹IFIC, Valencia-CSIC, and D.F.A.M.N., U. de Valencia, Avda. Dr. Moliner 50, E-46100 Burjassot (Valencia), Spain

⁵⁰Institut für Hochenergiephysik, Österr. Akad. d. Wissensch., Nikolsdorfergasse 18, A-1050 Vienna, Austria

⁵¹Inst. Nuclear Studies and University of Warsaw, Ul. Hoza 69, PL-00681 Warsaw, Poland

⁵²Fachbereich Physik, University of Wuppertal, Postfach 100 127, D-42097 Wuppertal 1, Germany

⁵³On leave of absence from IHEP Serpukhov

1 Introduction

The theory of strong interactions, QCD, does not provide reliable calculations of the transformation of the final state quarks and gluons into observed hadrons. This phase, called “hadronization”, is usually simulated using hadronization models. The measured particle production cross sections provide constraints and test the models available. Particles with high mass and spin may be produced more directly and so provide cleaner information.

In hadronic Z^0 decays, inclusive production rates have been measured for a large number of meson and baryon states (see Ref. [1] and references therein). However, up to now, the tensor meson $f'_2(1525)$ has been observed and studied only in exclusive reactions like $K^- p \rightarrow f'_2 \Lambda$ [2], $J/\psi \rightarrow f'_2 \gamma$ [3] and $\gamma\gamma \rightarrow f'_2$ [4]. Inclusive studies of this state are necessary for understanding the dynamics of its production.

This letter reports the first observation and inclusive analysis of $f'_2(1525)$ production in e^+e^- hadronic events at a centre-of-mass energy around 91.2 GeV. The measurement has been performed using data collected with the DELPHI detector at the LEP collider from 1992 to 1994.

The $f'_2(1525)$ has a mass of 1525 ± 5 MeV/ c^2 [5]. Its decay into K^+K^- (branching fraction 35.6%) was used in the present analysis.

2 Event Selection and Analysis

The DELPHI detector and its performance have been described in Refs. [6,7]. This analysis relied on the information provided by the tracking detectors: the Micro Vertex Detector (VD), the Inner Detector (ID), the Time Projection Chamber (TPC), the Outer Detector (OD) and the Forward Chambers (FCA, FCB), and by the Ring Imaging Cherenkov (RICH) detectors.

Charged particles were used if they had polar angle θ with respect to the beam axis between 25° and 155° , momentum p larger than 0.2 GeV/ c and smaller than 50 GeV/ c , measured track length in the TPC longer than 50 cm, and impact parameter with respect to the nominal beam crossing point less than 5 cm in the transverse plane and 10 cm along the beam direction. Hadronic events were selected by requiring that there were at least 5 such charged particles in the event, that the total energy of the charged particles exceeded 3 GeV in each of the two hemispheres defined with respect to the beam direction, that the total energy of all charged particles was larger than 15 GeV, that the total momentum unbalance was less than 30 GeV/ c , and that the polar angle of the thrust axis satisfied $|\cos \theta_{\text{th}}| < 0.75$.

The K^\pm identification relied on the Barrel RICH and Forward RICH detectors, imposing the “tight” selection criteria in the DELPHI algorithm HADSIGN [7]. Charged kaons were identified with an average purity of about 70% for momenta larger than 1.0 GeV/ c , as estimated from Monte Carlo simulation. In the 1994 data, for which both the liquid and the gas RICH were operational, 1,020,889 hadronic events were retained after the cuts. The number with at least two identified charged kaons was 300,821. Adding the data collected during 1992 and 1993, when the gas RICH was operational, increased the statistics for kaon pairs with $x_p > 0.22$, where $x_p \equiv 2p/\sqrt{s}$, by about 50%.

The detector effects on the analysis were estimated using the DELPHI simulation program DELSIM [7]. The events were generated using the JETSET 7.3 Parton Shower model [8] with parameters tuned to DELPHI data [9]. Production of the $f'_2(1525)$ was included.

The $f'_2(1525)$ signal in the K^+K^- mass distributions was described, both for the full measured x_p range and for separate intervals in x_p , by a relativistic Breit-Wigner function

$$BW(M, M_0, \Gamma_0) = \frac{M \cdot M_0 \cdot \Gamma(M)}{(M_0^2 - M^2)^2 + (M_0 \cdot \Gamma(M))^2}; \quad \Gamma(M) = \Gamma_0 \cdot \left(\frac{q}{q_0}\right)^{2L+1} \cdot \frac{2q_0^2}{q_0^2 + q^2} \quad (1)$$

where M is the K^+K^- mass, M_0 and Γ_0 are the mass and width of the $f'_2(1525)$ resonance, q and q_0 are the kaon momentum in the K^+K^- rest system for masses of M and M_0 respectively, and the angular momentum of the decay products L was set equal to 2. The background was parametrized by the function

$$BG(M, a_1, \dots, a_4) = a_1 + a_2M + a_3M^2 + a_4M^3. \quad (2)$$

In part of the analysis, a second resonance $f_J(1710)$ [5] decaying into K^+K^- was also included in the fitting procedure, using the same function as (1) with L set equal to 2, and neglecting possible interference between $f'_2(1525)$ and $f_J(1710)$.

Thus the K^+K^- invariant mass spectrum was fitted with the function

$$\alpha \cdot BW_{f'_2}(M, M_0^{f'_2}, \Gamma_0^{f'_2}) + \beta \cdot BW_{f_J}(M, M_0^{f_J}, \Gamma_0^{f_J}) + BG(M, a_1, \dots, a_4). \quad (3)$$

The resonance masses M_0 and widths Γ_0 were either left free in the fitting procedures, or were fixed at their values as measured in this experiment, or were fixed at their world average values [5] from the Particle Data Group (PDG). The K^+K^- mass distributions were fitted in the region from 1.3 to 2.0 GeV/ c^2 . The numbers of $f'_2(1525)$ candidates were determined by integrating the Breit-Wigner function in expression (3).

3 Results and Discussion

The K^+K^- invariant mass spectrum for identified charged kaon candidates is shown in Figure 1 for the 1994 data in the region $x_p > 0.05$. A clear $f'_2(1525)$ signal is observed. For the fit to the function (3) that is shown, the mass and width of the $f_J(1710)$ were set to the world averages, 1709 and 140 MeV/ c^2 respectively [5], and the parameters of the $f'_2(1525)$ were left free. The fit gave $M_0^{f'_2} = 1535 \pm 5$ MeV/ c^2 and $\Gamma_0^{f'_2} = 60 \pm 20$ MeV/ c^2 , to be compared with the PDG values of 1525 ± 5 and 76 ± 10 , respectively. The systematic errors on the measured mass and width, obtained by varying the background, were 4 MeV/ c^2 and 19 MeV/ c^2 respectively.

The measured K^+K^- invariant mass distributions in four x_p intervals are presented in Figure 2 together with the fits and the background. The 1992 and 1993 data are included for $x_p > 0.22$. The masses and widths of the $f'_2(1525)$ in the separate x_p intervals were fixed to the experimental values obtained above for the full $x_p > 0.05$ region.

In the lowest x_p region, $0.05 < x_p < 0.10$, a signal consistent with the $f_J(1710)$ state is seen. A fit to a $f_J(1710)$ signal with free mass in this x_p interval gave $M_{f_J} = 1690 \pm 11$ MeV/ c^2 , in reasonable agreement with the world average [5]. The number of $f_J(1710)$ candidates in this x_p interval obtained by a fit with the $f_J(1710)$ mass and width fixed at the PDG values was 405 ± 200 ($\chi^2/DF=29.3/43$). Excluding the $f_J(1710)$ increased the χ^2 by 5.6. It was also verified that in the simulation, although some structure from charm meson decays in the $f_J(1710)$ mass region was observed at higher x_p values, the production of states with higher masses, particularly the production of charmed mesons, did not generate an enhancement in the $f_J(1710)$ mass region in this lowest x_p interval.

However, the significance of the $f_J(1710)$ corresponds to only two standard deviations. The analysis was therefore repeated without accounting for this state, i.e. when fixing

$\beta = 0$ in function (3). The dashed line in Figure 1 shows the overall fit obtained. The dotted lines in Figure 2 show the backgrounds fitted in each x_p bin.

x_p interval	Number of $f'_2(1525)$		Average number	$\epsilon_\phi^r/\epsilon_{f'_2}^r$	$\langle N_{f'_2} \rangle$
	with f_J	without f_J			
0.05 – 0.10	419 ± 118	295 ± 105	357 ± 112	1.18	0.0050 ± 0.0017
0.10 – 0.22	561 ± 164	375 ± 147	468 ± 156	0.81	0.0074 ± 0.0026
0.22 – 0.50	186 ± 173	25 ± 141	106 ± 157	0.72	0.0012 ± 0.0018
0.50 – 1.00	109 ± 46	120 ± 50	115 ± 48	1.04	0.0023 ± 0.0010

Table 1: *Numbers of $f'_2(1525) \rightarrow K^+K^-$ candidates with and without including the $f_J(1710)$ in the fit, the average of those two numbers, the ratio $\epsilon_\phi^r/\epsilon_{f'_2}^r$ of the reconstruction efficiencies for ϕ and f'_2 decays into K^+K^- , and the resulting average $f'_2(1525)$ multiplicity per hadronic Z^0 decay in the four x_p intervals, corrected for unobserved decay modes.*

The numbers of $f'_2(1525)$ obtained in the four x_p intervals are presented in Table 1. The averages of the numbers obtained with and without the $f_J(1710)$ were used for the subsequent analysis, and half the difference between these numbers was taken into account as a systematic error. In the region $0.22 < x_p < 0.50$, the number of $f'_2(1525)$ candidates depended slightly on the range used for the fitted mass distribution. The differences between the fit results were also taken into account in the systematic error.

In order to measure the average multiplicity and x_p distribution of the $f'_2(1525)$, the rates were expressed relative to the ϕ production rates by:

$$\langle N_{f'_2}^r \rangle = \langle N_\phi^r \rangle \frac{N_{f'_2}^r}{N_\phi^r} \cdot \frac{\epsilon_\phi^r}{\epsilon_{f'_2}^r}, \quad (4)$$

where $\langle N_{f'_2}^r \rangle$ and $\langle N_\phi^r \rangle$ are the mean multiplicities, $N_{f'_2}^r$ and N_ϕ^r the numbers of reconstructed decays, and $\epsilon_{f'_2}^r$ and ϵ_ϕ^r are the efficiencies, for $f'_2(1525)$ and $\phi(1020)$ respectively. All numbers in Eq. (4) correspond to the numbers reconstructed in the K^+K^- decay mode, indicated by the superscript r , both for $f'_2(1525)$ and $\phi(1020)$. The N_ϕ^r were obtained using the same K^+K^- mass distributions as the $N_{f'_2}^r$, and a similar fitting procedure.

The average of the $\phi(1020)$ production rates measured by the LEP experiments [10] is 0.107 ± 0.009 per hadronic Z^0 decay [1]. As the tuned JETSET model yields a good description of the momentum spectrum of the $\phi(1020)$, the relative $\phi(1020)$ multiplicities in the four x_p regions were calculated from JETSET, while the global ϕ multiplicity was renormalized to the above average value measured at LEP. The systematic errors on the numbers and average multiplicities of the ϕ were taken into account, as was the branching fraction of ϕ into K^+K^- (49.1%).

The use of Eq. (4) for measuring the average $f'_2(1525)$ multiplicities avoided the calculation of the kaon efficiency from the simulation: the efficiency ratio $\epsilon_\phi^r/\epsilon_{f'_2}^r$ could be extracted more reliably from the simulation than $\epsilon_{f'_2}^r$ itself.

The efficiency ratio was calculated from simulated events for the full measured x_p interval, $\epsilon_\phi^r/\epsilon_{f'_2}^r=0.87$, and for the four x_p regions. In each region of x_p , the average of two $\epsilon_\phi^r/\epsilon_{f'_2}^r$ ratios, one for the full measured x_p interval and the other for the given x_p region, was used. The efficiency ratios are given in Table 1. The statistical errors on these numbers are negligible. Their systematic errors were taken into account.

The average $f'_2(1525)$ multiplicities, $\langle N_{f'_2} \rangle$, in four x_p intervals, calculated using Eq. (4) and corrected for unobserved $f'_2(1525)$ decay modes, are given in the last column of Table 1. The measured average multiplicity in the $x_p > 0.05$ range, obtained by summing over the four x_p intervals, amounted to 0.0159 ± 0.0037 (stat) per hadronic event. The extrapolation to the full x_p range, assuming that the unmeasured interval $x_p < 0.05$ is represented by the normalized JETSET 7.3 PS model tuned to DELPHI data [9], yielded the final value for the total $f'_2(1525)$ multiplicity

$$\langle N_{f'_2} \rangle = 0.020 \pm 0.005 \text{ (stat)} \pm 0.006 \text{ (syst)}. \quad (5)$$

The systematic error quoted is the quadratic sum of the following uncertainties.

- The fitting with and without the $f_J(1710)$ contributed an error of ± 0.0041 .
- The uncertainty on the ratio of the efficiencies and the numbers and average multiplicities of the ϕ was estimated by recalculating the average f'_2 multiplicities using the expression

$$\langle N_{f'_2} \rangle = N_{f'_2}^r / (N_{ev} \cdot \epsilon_{f'_2}^r) \quad (6)$$

(where N_{ev} is the number of hadronic Z decays), which does not make use of the ϕ multiplicities, and taking the $f'_2(1525)$ efficiencies, $\epsilon_{f'_2}^r$, from simulation. The difference in the average $f'_2(1525)$ multiplicities obtained from Eq. (4) and Eq. (6) was 0.0031; this difference was considered as a systematic error.

- The fitting function and the mass and width of the signal were varied. As an alternative shape of the f'_2 signal, the shape from simulated events was considered. As input value for the mass and width of the f'_2 , the PDG values, 1525 and 76 MeV/ c^2 respectively, were chosen. The analysis of simulated events did not show evidence of a distortion of the Breit-Wigner shape of the f'_2 due to the influence of phase space and detector effects: no mass shift was observed and the width was increased by the value of the K^+K^- mass resolution; this was almost constant at about 10 MeV/ c^2 over the full measured $x_p > 0.05$ range. The error from these sources was estimated to be ± 0.0017 .
- The reflections from other states in the f'_2 mass region was calculated from events generated according to the JETSET model and passed through detector simulation, and were subtracted from the experimental K^+K^- mass distributions. All states decaying into two or more charged particles which were identified after the detector simulation as an unlike-sign kaon pair were considered. The corresponding error was estimated to be ± 0.0017 .
- The correction for the unmeasured interval $x_p < 0.05$ based on the JETSET 7.3 PS model amounted to 0.0043; an error of ± 0.0014 (one third) was assigned to it.

The observed ratio

$$\sigma(f'_2(1525))/\sigma(\phi(1020)) = 0.19 \pm 0.07 \quad (7)$$

agrees with the ratio

$$\sigma(f_2(1270))/\sigma(\rho^0(770)) = 0.24 \pm 0.07 \quad (8)$$

measured in [11], as well as with the average ratio of tensor to vector mesons in hadronic reactions of 0.25 ± 0.03 [12].

Table 2 and Figure 3 give the differential cross sections of $f'_2(1525)$ as a function of x_p . The dashed line in Figure 3 shows the $\phi(1020)$ production as modelled by JETSET and normalized to the mean $\phi(1020)$ multiplicity measured at LEP [1]. The shapes of the x_p distributions of the $f'_2(1525)$ and $\phi(1020)$ are in agreement within the large errors,

x_p interval	$(1/\sigma_h) \cdot d\sigma/dx_p$
0.05 - 0.10	$0.100 \pm 0.034 \pm 0.032$
0.10 - 0.22	$0.062 \pm 0.022 \pm 0.024$
0.22 - 0.50	$0.004 \pm 0.006 \pm 0.006$
0.50 - 1.00	$0.005 \pm 0.002 \pm 0.002$

Table 2: *Differential cross section $(1/\sigma_h) \cdot d\sigma/dx_p$ for the production of $f'_2(1525)$. The first error is statistical and the second is systematic.*

but some indication of an increasing ratio of tensor to vector production (up to one) for the leading mesons in the high x_p region may also be seen, as observed previously in Ref. [11].

The measured average multiplicity and the x_p distribution of the $f'_2(1525)$ can be compared with the JETSET 7.3 model tuned to DELPHI data [9]. Parameters which are important for $f'_2(1525)$ production in the model are the strangeness suppression factor and the probability of strange tensor meson production; these were set to 0.28 and 0.132, respectively. The predicted value for the $f'_2(1525)$ average multiplicity in JETSET is 0.024, in good agreement with the measured value. The JETSET model also describes the x_p distribution well (Figure 3). Note that the JETSET model was tuned to DELPHI data for production of other mesons and baryons without using the present results on $f'_2(1525)$ production.

4 Conclusions

The first observation of $f'_2(1525)$ production in hadronic Z^0 decays has been reported. The production rate per hadronic Z^0 decay:

$$\langle N_{f'_2} \rangle = 0.020 \pm 0.005 \text{ (stat)} \pm 0.006 \text{ (syst)}$$

and the x_p distribution have been measured. The ratio of cross sections $f'_2(1525)/\phi(1020)$ is in agreement with the vector-to-tensor meson ratios measured for other states. The shapes of the x_p distributions for $f'_2(1525)$ and $\phi(1020)$ are similar, indicating similar production mechanisms of these mesons. The average multiplicity agrees well with the prediction of the JETSET model with DELPHI tuned parameters. The shape of the x_p spectrum is consistent with the one predicted by JETSET. The results of the inclusive analysis are consistent with the assumption that the $f'_2(1525)$ is a $s\bar{s}$ tensor meson.

Acknowledgements

We are greatly indebted to our technical collaborators and to the funding agencies for their support in building and operating the DELPHI detector, and to the members of the CERN-SL Division for the excellent performance of the LEP collider.

References

- [1] A. De Angelis, “Light quark hadrons in hadronic Z decays”, CERN-PPE/95-135, to be published in the Proceedings of the EPS-HEP Conference, Brussels 1995.
- [2] M. Aguilar-Benitez et al., *Z. Phys.* **C8** (1981) 313;
T. Armstrong et al., *Nucl. Phys.* **B224** (1983) 193.
- [3] DM2 Collaboration, J.E. Augustin et al., *Phys. Rev. Lett.* **60** (1988) 2238;
Mark 3 Collaboration, R.M. Baltrusaitis et al., *Phys. Rev.* **D35** (1987) 2077.
- [4] L3 Collaboration, M. Acciarri et al., *Phys. Lett.* **B363** (1995) 118, and references 2 and 14 therein.
- [5] Particle Data Group, *Phys. Rev.* **D50** (1994) 1173.
- [6] DELPHI Collaboration, P. Aarnio et al., *Nucl. Instr. Methods* **A303** (1991) 233.
- [7] DELPHI Collaboration, P. Abreu et al., “Performance of the DELPHI Detector”, CERN-PPE/95-194, to be published in *Nucl. Instr. Methods* **A**.
- [8] T. Sjöstrand, *Comp. Phys. Comm.* **27** (1982) 243; **28** (1983) 229; **39** (1986) 347;
T. Sjöstrand and M. Bengtsson, *Comp. Phys. Comm.* **43** (1987) 367.
- [9] DELPHI Collaboration, “Tuning and Test of Fragmentation Models Based on Identified Particles and Precision Event Shape Data”, Contributed paper eps0548 to the EPS-HEP Conference, Brussels 1995.
- [10] OPAL Collaboration, R. Akers et al., *Z. Phys.* **C68** (1995) 1;
ALEPH Collaboration, D. Buskulic et al., CERN-PPE/95-100;
DELPHI Collaboration, “Inclusive Production of $\phi(1020)$ in the Z Hadronic Decays at LEP”, Contributed paper eps0556 to the EPS-HEP Conference, Brussels 1995.
- [11] DELPHI Collaboration, P. Abreu et al., *Z. Phys.* **C65** (1995) 587.
- [12] DELPHI Collaboration, P. Abreu et al., *Phys. Lett.* **B298** (1993) 236.

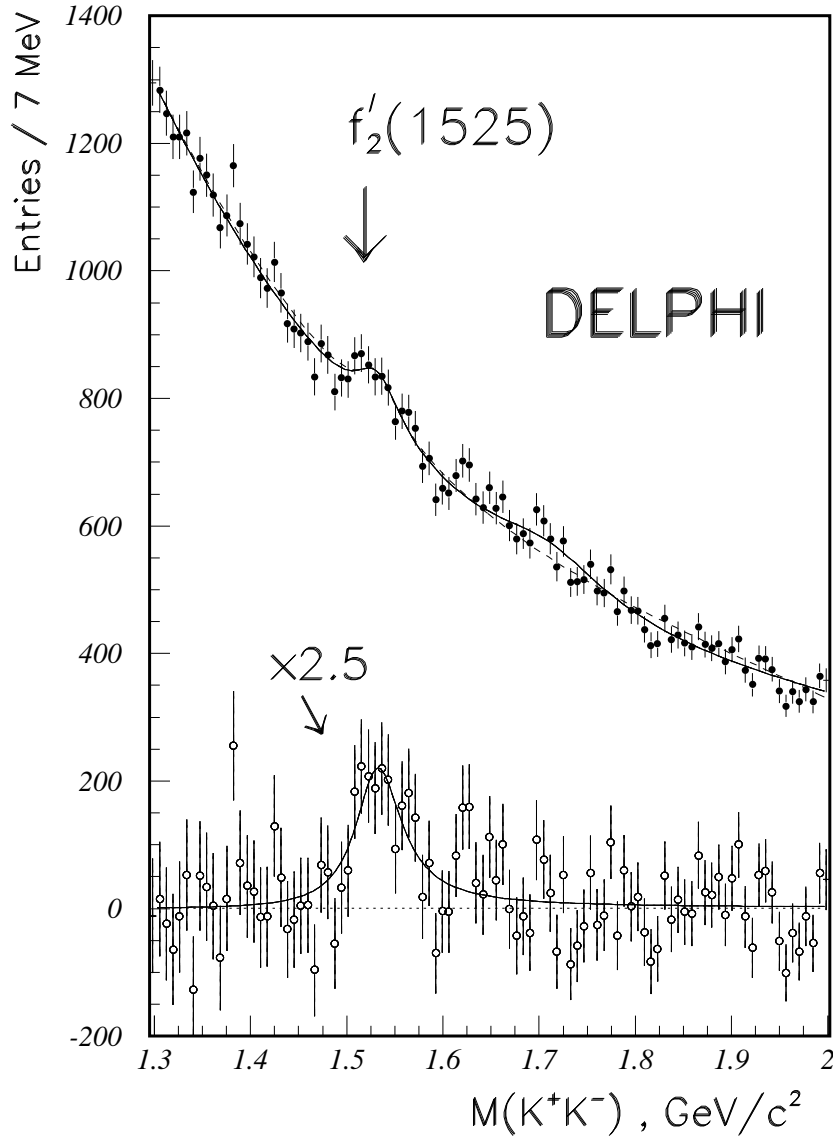


Figure 1: The K^+K^- invariant mass spectrum in the $f'_2(1525)$ mass region for the measured x_p interval $x_p > 0.05$, for the 1994 data. The full curve is the result of the fit to expression (3). The lower part of the Figure presents the data and the fit for $f'_2(1525)$ after subtracting the background and the $f_J(1710)$ contribution and multiplying by a factor 2.5. The dashed curve is the result of the fit to function (3) with $\beta = 0$.

DELPHI

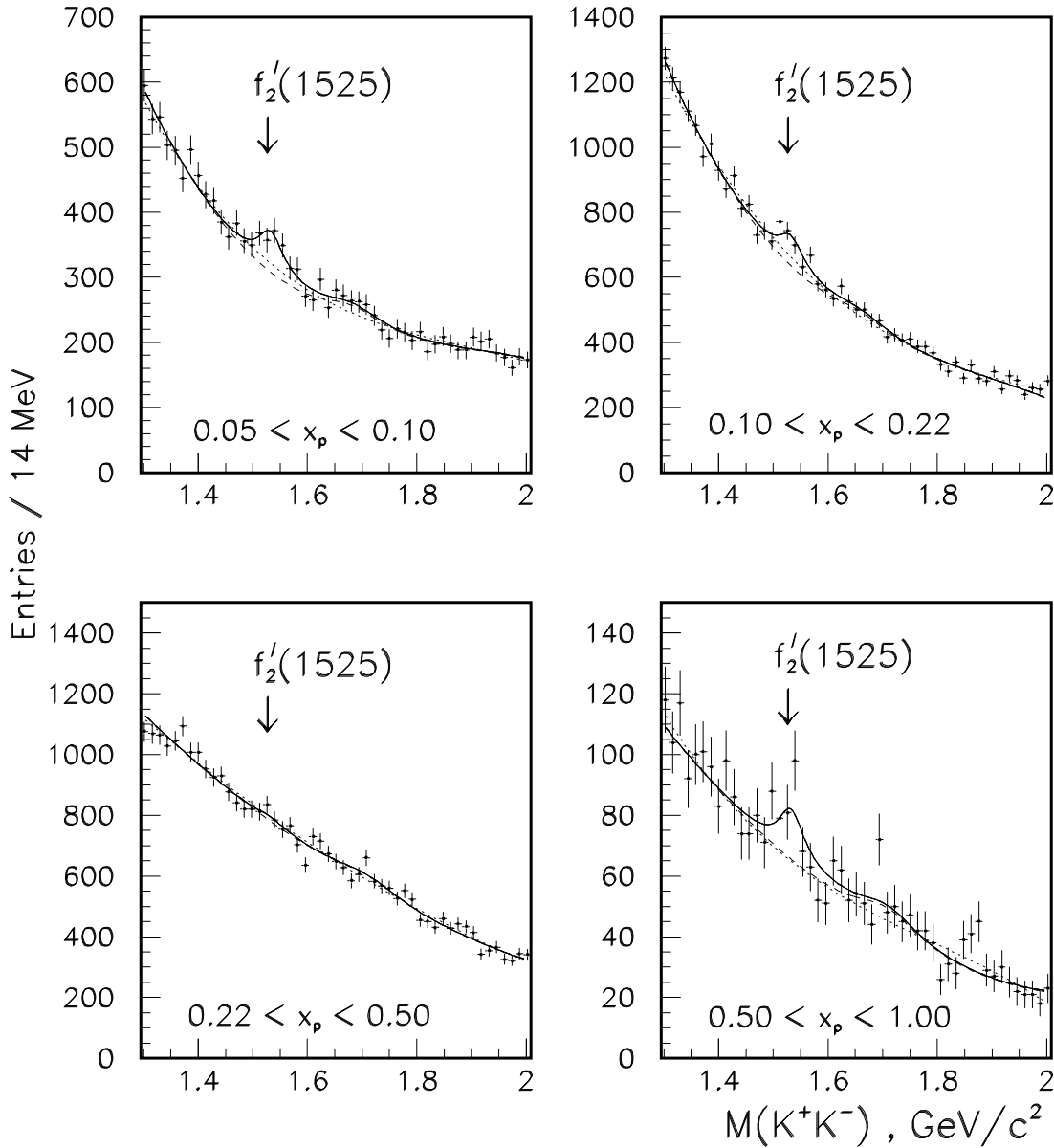


Figure 2: The K^+K^- invariant mass spectra in the $f_2'(1525)$ mass region for the x_p intervals indicated. The full curves show the fit to expression (3); the dashed curves represent the sum of background and the contribution of the $f_J(1710)$. The dotted curves show the background for the fit with $\beta = 0$ in function (3). The upper Figures are for the 1994 data while the lower Figures are for the combined 1992, 1993 and 1994 data.

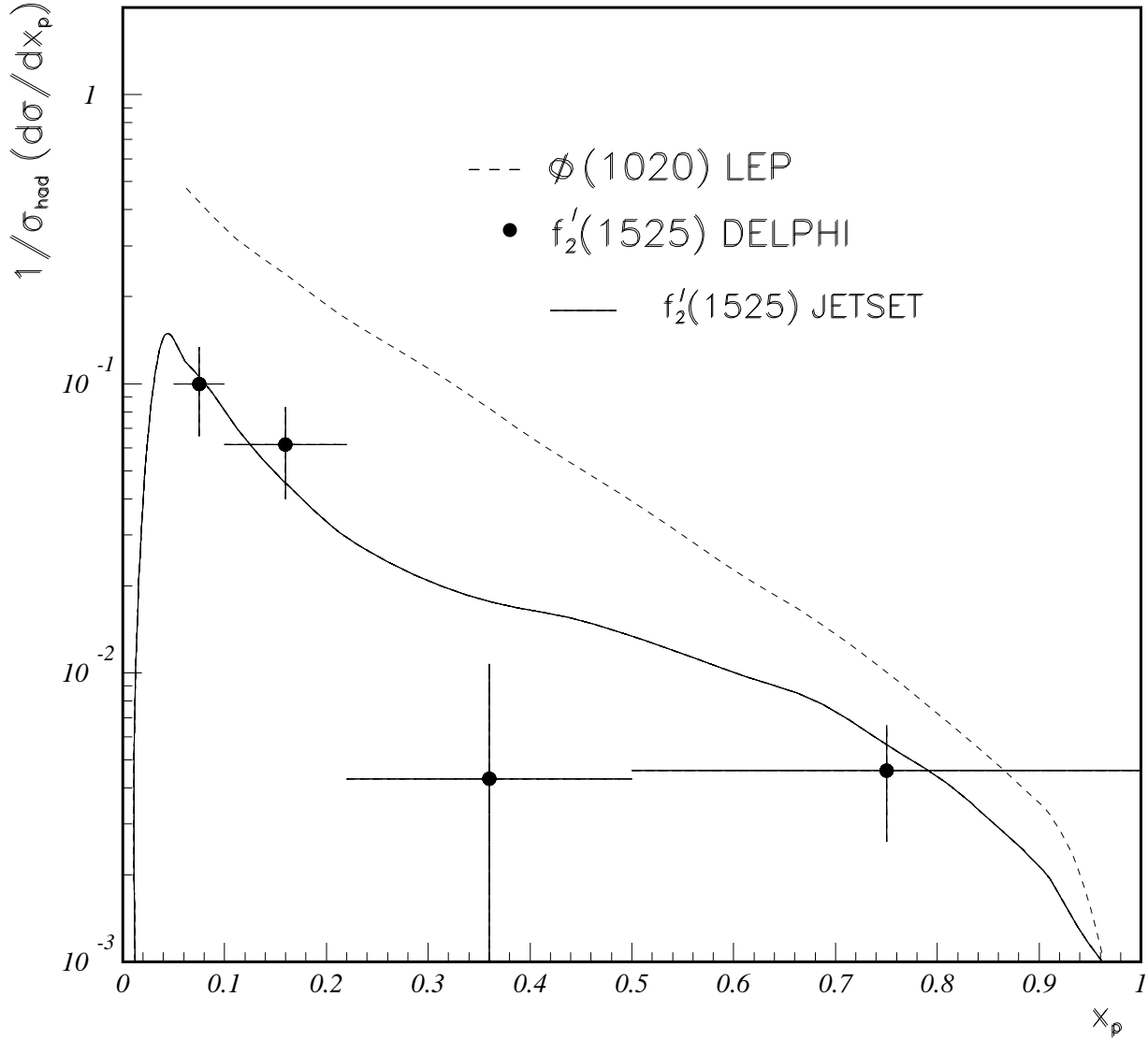


Figure 3: Differential cross section $(1/\sigma_h) \cdot d\sigma/dx_p$ for inclusive $f'_2(1525)$ production. Errors are statistical only. The dashed line shows the differential cross section $(1/\sigma_h) \cdot d\sigma/dx_p$ for $\phi(1020)$ production at LEP, the shape being taken from JETSET (see text). The full curve represents the expectation for the $f'_2(1525)$ from the JETSET 7.3 PS model with parameters tuned to other DELPHI data.